

Exotic phase transitions in RERhSn compounds

Kazimierz Łątka,
Roman Kmiec,
Robert Kruk,
Andrzej W. Pacyna,
Michał Rams,
Tobias Schmidt,
Rainer Pöttgen

Abstract Crystal and magnetic properties of three equiatomic ternary RERhSn compounds (where RE = Ce, Nd, Gd) have been studied by means of X-ray diffraction, ac, and dc magnetic susceptibility measurements, as well as using Mössbauer spectroscopy with ^{119}Sn and ^{155}Gd resonances. CeRhSn does not order magnetically down to 2 K while NdRhSn undergoes ferromagnetic transition at $T_C = 10.3$ K and GdRhSn orders antiferromagnetically below $T_N = 16$ K. Our CeRhSn and NdRhSn samples become superconductive below 6.5 K and 6.9 K, respectively.

Key words magnetic properties • phase transitions • Mössbauer spectroscopy

Introduction

Ternary equiatomic RERhSn stannides, where RE stands for rare earth element, with ZrNiAl type of structure have recently been extensively studied, mainly due to their interesting magnetic and electrical properties [4–6]. Some results were reported by Routsis *et al.* on Ce, Nd [6] and Gd [5] compounds. For CeRhSn magnetic susceptibility measurements were done from 4.2 K to about 120 K where the Curie-Weiss law was not found [6]. No magnetic ordering was discovered for NdRhSn [6] and GdRhSn which appeared to be antiferromagnetic below $T_N = 14.8$ K [5]. Results of ^{119}Sn Mössbauer studies for GdRhSn were reported for the first time by Dwight *et al.* [1]. However, resonance spectra were not presented there and the suggestion that this compound may be magnetic above 77.3 K is definitely wrong. Also, the obtained value for hyperfine magnetic field $H_{\text{eff}} = 3.9$ kOe at 4.2 K is much smaller than the value found in this work.

In the present paper, we focus our attention on the three representatives of the RERhSn family just mentioned above, namely CeRhSn, NdRhSn, and GdRhSn compounds. The last compound is taken as a reference material owing to the fact that the $4f^7$ shell of Gd has S-character and thus crystalline electric field effects can be neglected in this case. Detailed magnetic measurements were performed in ac (alternating current) and dc (direct current) modes using a 7225 Lake Shore susceptometer/magnetometer as well as utilising a superconducting quantum interference device (SQUID – Quantum Design) magnetometer on powder samples. Application of external magnetic field together with the studies of higher harmonics allowed for a better determination and understanding of the observed phase transitions of different origin. The local properties were investigated by means of Mössbauer spectroscopy employing ^{119}Sn gamma resonance 23.875 keV transition as well as ^{155}Gd 86.5 keV resonance in the case of GdRhSn sample.

K. Łątka✉, M. Rams
Marian Smoluchowski Institute of Physics,
Jagiellonian University,
4 Reymonta Str., 30-059 Kraków, Poland,
Tel.: +48 12/ 632 48 88 ext. 5668, Fax: +48 12/ 633 70 86,
e-mail: uflatka@cyf-kr.edu.pl

R. Kmiec, R. Kruk, A. W. Pacyna,
The Henryk Niewodniczański Institute of Nuclear Physics,
152 Radzikowskiego Str., 31-342 Kraków, Poland

T. Schmidt, R. Pöttgen
Institut für Anorganische und Analytische Chemie,
Universität Münster,
8 Wilhelm-Klemm-Str., 48149 Münster, Germany

Received: 17 July 2002, Accepted: 5 December 2002

Experimental

Synthesis of CeRhSn compound and X-ray diffraction analysis have been carried out in a similar way as it was previously described in Ref. [4]. Magnetic properties were studied on a powder sample in a wide temperature range between 2 K and 293 K with the help of several ac and dc magnetic susceptibility methods using commercial 7225 Lake Shore and SQUID (Quantum Design) magnetometers. Preliminary resistivity measurements were made for Ce and Nd compounds on pressed powder probes utilising a standard four contact technique owing to the lack of bulk samples. Standard equipment was used for ^{119}Sn and ^{155}Gd Mössbauer investigations. Recorded spectra were analysed within Lorentzian approximation in the case of tin spectroscopy and by means of transmission integral for gadolinium resonance using a numerical diagonalisation of the full hyperfine interaction Hamiltonian H_{hf} . The ^{119}Sn resonance spectra obtained for NdRhSn below T_C were analysed employing the Wivel and Mørup method [8] to account for a distribution of the magnetic hyperfine fields. As a rule, in the fitting procedure of magnetically split spectra, the number of independently fitted parameters were reduced by constraining the absolute value of the quadrupole constant $|\Delta E_Q = eQV_{zz}|$ and the corresponding value of half-width Γ to those obtained above the magnetic transition temperature.

Results and discussion

X-ray studies

X-ray diffraction studies have been performed on powder samples as well as single crystals of RERhSn (RE = Ce, Nd, Gd) compounds. The structure refinement indicates that all these stannides crystallize in ZrNiAl type of structure with space group $P62m$. In contrast to the data reported by Routsis *et al.* [6], anomalous unit-cell volume of CeRhSn was confirmed in relation to that shown by other members of RERhSn series [4] indicating Ce valence-fluctuating behaviour.

Magnetic and transport properties

The high-temperature magnetic susceptibilities of the all three investigated compounds follow the modified Curie-Weiss law in the form: $\chi = \chi_0 + C/(T - \Theta_p)$ where χ_0 is the temperature independent term, C is the Curie constant, and Θ_p is the paramagnetic Curie temperature. It was found [3] that for the CeRhSn compound the derived magnetic effective moment is much reduced in comparison to the theoretical value characteristic for a free Ce^{3+} ion (in $^2F_{5/2}$ ground state) described by $\mu_{\text{eff}}^{(\text{th})} = g_J \mu_B [J(J+1)]^{1/2} = 2.54 \mu_B$. This gives another hint for an intermediate valence (IV) behaviour of cerium [3]. The negative value of $\Theta_p = -70$ K revealed antiferromagnetic correlations.

Numerical calculations clearly show that the Sales-Wohleben (S-W) model [7] does not describe properly the temperature dependence of the magnetic susceptibility. The magnetic effective moments determined for NdRhSn ($3.04 \mu_B$) and GdRhSn ($7.2 \mu_B$) compounds are lower than

the values of free Nd^{3+} ($3.62 \mu_B$) and Gd^{3+} ($7.94 \mu_B$) ions, respectively. The obtained paramagnetic Curie temperatures Θ_p are positive and equal to 9.1 K (Nd) and 26 K (Gd); pointing to the existence of ferromagnetic interactions in both compounds.

In contrary to the Ce compound which does not order magnetically down to 2 K (Fig. 1), NdRhSn shows ferromagnetic character with Curie temperature $T_C = 10.3$ K (Fig. 1), while GdRhSn undergoes antiferromagnetic transition at $T_N = 16$ K (Fig. 2) in good agreement with the value $T_N = 14.8$ K given in Ref. [5]. Non zero values of the second and third harmonics registered by ac methods for last two compounds are in accord with ferromagnetic transition observed for Nd sample indicating simultaneously non-collinear character of antiferromagnetic ordering of Gd moments in GdRhSn compounds. This observation is likely due to a magnetic frustration expected for triangular coordination symmetry of the Gd magnetic ions.

Superconductivity of CeRhSn and NdRhSn samples

The onset of superconductivity is observed by a sudden diamagnetic drop of the dc susceptibility and the fall of

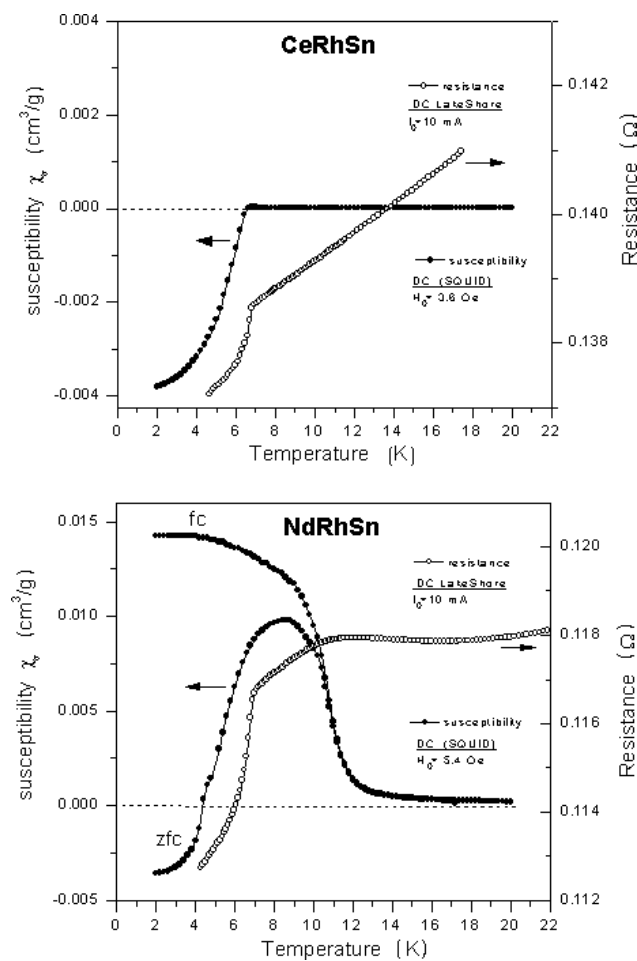


Fig. 1. Temperature dependencies of the resistivity (right hand scale), and the DC magnetic susceptibility as obtained by SQUID (left hand scale); measured on the pressed powder pellets of our CeRhSn (top) and NdRhSn (bottom) samples. The samples were first cooled down in zero magnetic field and susceptibility measurements were done with rising temperature in the magnetic field of 3.6 Oe (CeRhSn) and 5.4 Oe (NdRhSn), respectively.

resistivity (Fig. 1) for our CeRhSn ($T_c = 6.5$ K) and NdRhSn ($T_c = 6.9$ K) samples. Superconducting transition is also confirmed for both samples by kinks at χ' and dissipative peaks at χ'' and also by strong signals shown by third harmonic at temperatures which are very close to those given above. Simultaneously signals of the second harmonic measured for these samples are zero. Additionally, superconducting state is reflected by characteristic hysteresis loops below T_c (Fig. 3). However, the superconducting fractions were estimated from magnetic measurements not exceeding about 10% (without taking into account demagnetisation factor) for both cases.

Mössbauer spectroscopy

^{119}Sn and ^{155}Gd Mössbauer spectra for RERhSn (RE = Ce, Nd, Gd) compounds are displayed in Figs. 4–7. Tables 1 and 2 present hyperfine parameters obtained in the high and low temperature regions i.e. in paramagnetic and magnetic states, respectively. Owing to the non-cubic and low local symmetry ($m2m$) of the Sn and Gd crystallographic positions magnetically split spectra can be fitted in a reliable but approximate way assuming collinear magnetic structure. In that case, if magnetic moments are not parallel to the c-axis, the spectrum consists of three subspectra characterised by the same relative intensities, and the same magnitudes of hyperfine magnetic and quadrupole parameters but with the different values of θ or ϕ (or both) angles, specifying the orientation of hyperfine magnetic

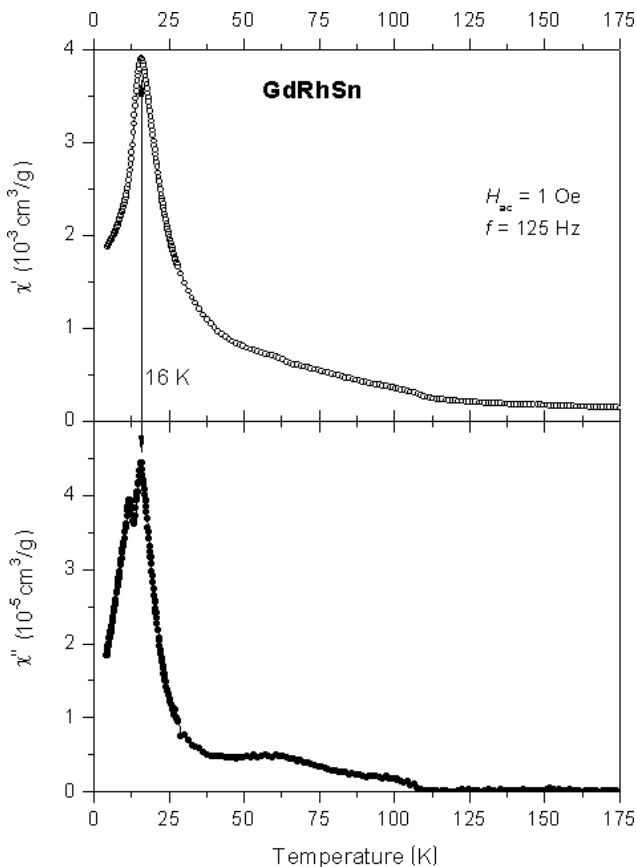


Fig. 2. GdRhSn zero-field susceptibilities χ' and χ'' recorded simultaneously as a function of temperature with the amplitude of the oscillating field $H_{ac} = 1$ Oe at the internal frequency $f = 125$ Hz.

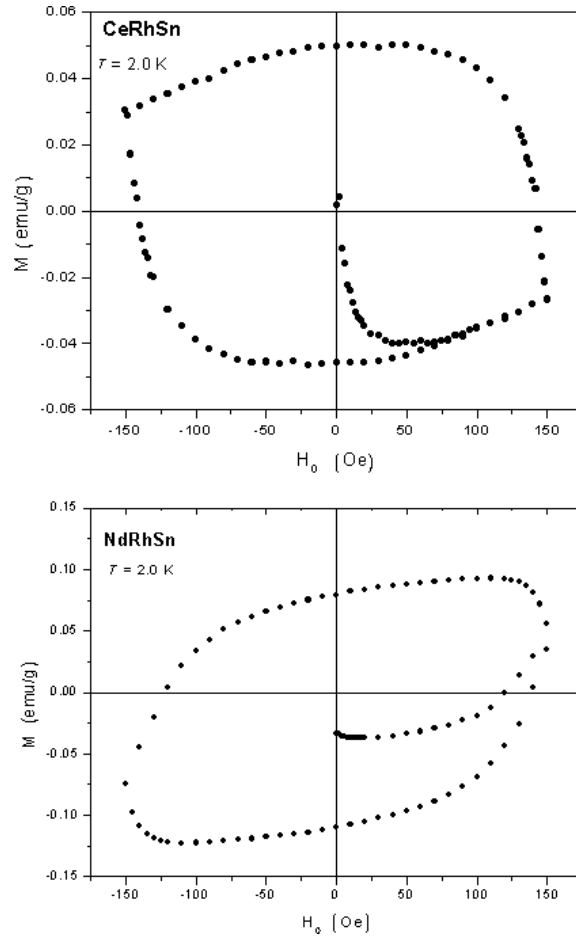


Fig. 3. Virgin magnetisations and low-field hysteresis loops at $T = 2$ K observed for our CeRhSn (top) and NdRhSn (bottom) samples.

field H_{eff} direction with respect to the principal axes of the electric field gradient (EFG) tensor, for three different positions of tin or gadolinium [2]. If the magnetic moments are perpendicular to the c-axis and V_{zz} is in the basal plane the three individual θ angles are mutually related as θ , $\theta + 120^\circ$ and $\theta + 240^\circ$ while the azimuthal ϕ angle has to be 0° or 90° (see extended discussion on that problem in Ref. [2]). A single component in the resonance spectrum

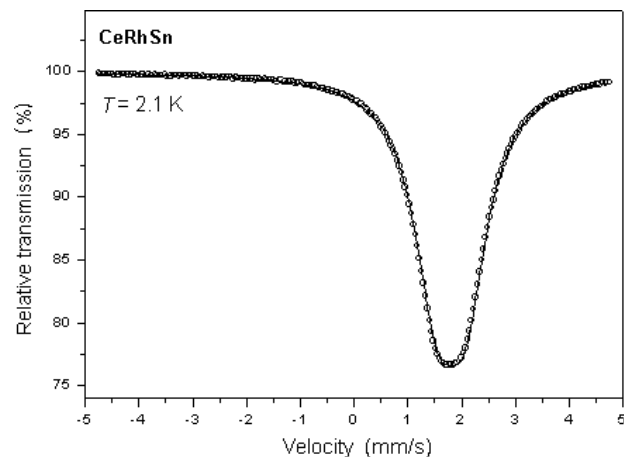


Fig. 4. ^{119}Sn resonance spectrum for CeRhSn at 2.1 K. The continuous line represents the least-squares fit to the experimental points.

| T (K) | H_{eff} (kOe) | eQV_{zz} (mm/s) | δ_{is} (mm/s) | Γ (mm/s) | θ (deg) | χ^2 | AR (%) |
|------------|---------------------------|----------------------|--------------------------------|--------------------|-------------------|----------|-----------|
| CeRhSn | | | | | | | |
| 2.1 | – | –1.10(1) | 1.82(1) | 1.04(1) | – | 2.79 | |
| 293 | – | 1.09(1) | 1.81(1) | 0.89(1) | – | 1.28 | |
| NdRhSn | | | | | | | |
| 1.85 | 66.5(1) | –1.27* | 1.796(2) | 0.89* | 96(2) | 2.1 | |
| 293 | – | 1.18(1) | 1.785(1) | 0.89(1) | – | 2.9 | |
| GdRhSn | | | | | | | |
| 1.8 | 15(1) | 0.997* | 1.762(2) | 1.26(1) | 54(1) | 0.89 | 89 |
| | – | 0.46(6) | 1.762(2) | 0.9* | – | 11 | |
| 293 | – | 0.997(4) | 1.751(2) | 0.86(1) | – | 1.69 | 89* |
| | – | 0.46* | 1.751(2) | 0.9* | – | | 11* |

*Parameter kept constant during the fit.

Table 1. Hyperfine interaction parameters inferred from ^{119}Sn resonance spectra obtained for RERhSn (RE = Ce, Nd, Gd) intermetallic compounds at the lowest temperatures as indicated and at room temperature (293 K).

Table 2. Hyperfine interaction parameters inferred from the ^{155}Gd resonance spectra obtained for the GdRhSn intermetallic compound at 4.2 K and 20 K.

| T (K) | H_{eff} (kOe) | eQV_{zz} (mm/s) | δ_{is} (mm/s) | η (mm/s) | Γ_A (deg) | θ_1 (deg) | θ_2 (deg) | θ_3 | χ^2 |
|------------|---------------------------|----------------------|--------------------------------|------------------|---------------------|---------------------|---------------------|------------|----------|
| 4.2 | 208(3) | –2.642* | 0.351(3) | 0.36(6) | 0.40(2) | 4(9) | 131(3) | 96(8) | 0.83 |
| 20 | – | 2.642(8) | 0.338(2) | – | 0.36(1) | – | – | – | 1.3 |

*Parameter kept constant during the fit.

can be expected only when H_{eff} is parallel to the c-axis independently of the direction of the principal axis V_{zz} .

^{119}Sn Mössbauer spectroscopy

For Ce compound no magnetic splitting down to 2 K (see Fig. 4) is observed for ^{119}Sn spectra. Because of the poor resolution and relatively small magnetic splitting of the spectra obtained for other investigated compounds at the lowest temperatures, the asymmetry parameter $\eta = (V_{xx} - V_{yy})/V_{zz}$ was put to zero during the fitting procedure. The resonance ^{119}Sn spectra of NdRhSn, below its ferromagnetic transition, can be effectively fitted with one θ value (see Table 1) assuming distribution of magnetic hyperfine fields as illustrated in Fig. 5. This distribution broadens very much with rising temperature towards T_C . We prescribed tentatively such a distribution to a helical magnetic ordering of Nd magnetic moments. If one supposes that Nd moments lie on a cone close to the c-axis, changing azimuthal angles from plane to plane then it should result in different hyperfine transferred fields seen by Sn atoms. Temperature dependent change of Nd magnetic moment directions should lead, in turn, to a broadening of hyperfine magnetic field distribution observed in fact experimentally. To get proper fit of GdRhSn spectra detected at 1.8 K and 293 K (Fig. 6), the second non-split component having a smaller quadrupole interaction constant (Table 1) with intensity of about 11% (taken from area ratio – AR at 1.8 K, see Table 1) must be included. This paramagnetic contribution can come from Sn atoms located at one of Rh sites with smaller ΔE_Q .

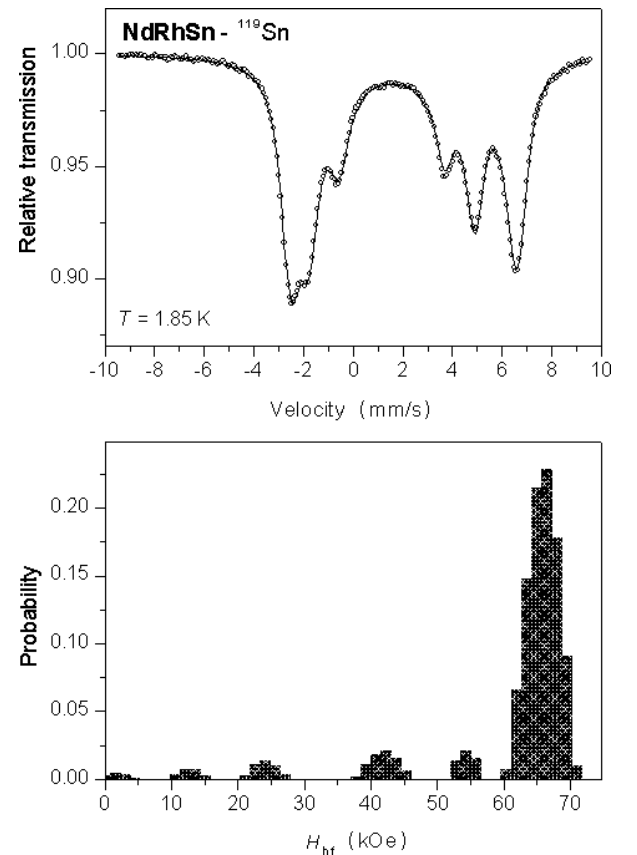


Fig. 5. ^{119}Sn resonance spectrum for NdRhSn at 1.85 K (top) and the respective distribution curve $P(H_{\text{eff}})$ (bottom). The continuous line represents the least-squares fit to the experimental points.

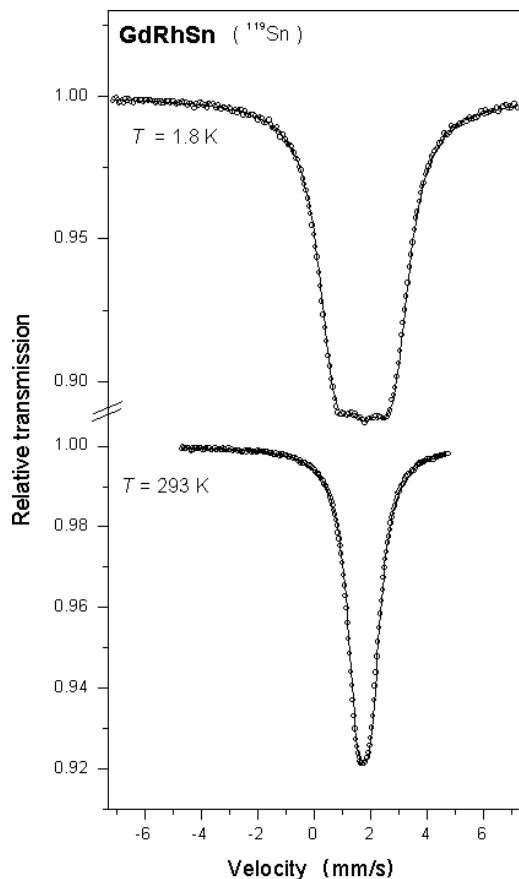


Fig. 6. ^{119}Sn resonance spectra for GdRhSn obtained at 1.8 K and 293 K. The continuous lines represent the least-squares fits to the experimental points.

^{155}Gd Mössbauer spectroscopy

Numerical simulations showed that the best fit to the ^{155}Gd spectrum registered at 4.2 K (Fig. 7) can be obtained with parameters listed in Table 2. It is seen that only two of three θ angles are related in the way described above, while the third angle does not keep this relation what can be another hint for Gd magnetic moments frustration. Here, V_{zz} axis of the EFG and magnetic moments were assumed to lie in basal plane perpendicular to the c -axis while V_{yy} is directed along this axis. The derived from ^{155}Gd Mössbauer spectra of GdRhSn V_{zz} and η parameters allowed us to estimate the quadrupolar B_2^0 and B_2^2 factors in the crystalline electric field (CEF) Hamiltonian $H = \sum B_n^m O_n^m$, for rare earth elements with non zero orbital momentum including cerium. Taking into account truncated Hamiltonian, limited to only two first terms as leading components we have shown that CEF has a minor effect on the reduction of μ or μ_{eff} for CeRhSn compound. Therefore, it seems that influence of the CEF in the Ce demagnetisation can be neglected. From negative values of B_2^0 and B_2^2 parameters calculated for Nd ion one can anticipate that magnetic moments of Nd should be ordered along or close to the c -axis what justifies our fitting assumptions.

Conclusions

Antiferromagnetic ordering was confirmed for GdRhSn, but in contrary, ferromagnetic arrangement was found for

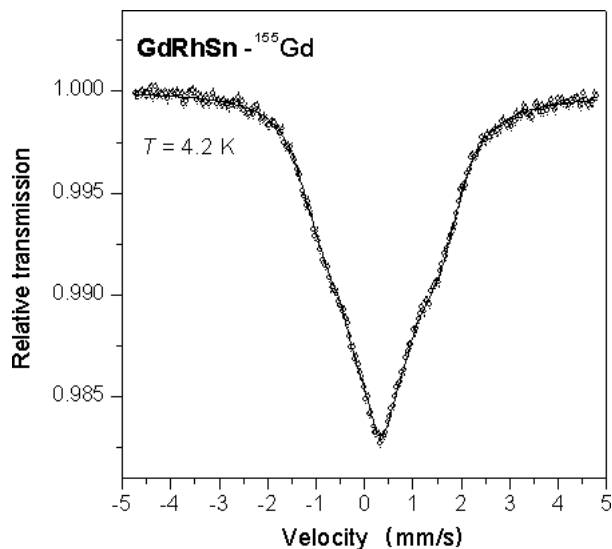


Fig. 7. ^{155}Gd resonance spectrum for GdRhSn at 4.2 K. The continuous line represents the least-squares fit to the experimental points.

NdRhSn while CeRhSn does not order magnetically up to 2 K and its reduced magnetic moment as well as anomalous volume deviation from usual lanthanide contraction point to the valence instability of this last compound. The observed reduction of the effective magnetic moment observed for CeRhSn cannot be explained by crystalline field effects or by application of S-W ICF model [7]. Diamagnetic behaviour of our CeRhSn and NdRhSn samples and the observed drops of their resistivities at the lowest temperatures investigated are the most exciting phenomena being characteristic for superconducting state. This aspect needs further detailed investigations. Pure quadrupole split ^{119}Sn Mössbauer spectra were observed for CeRhSn down to 2 K, while NdRhSn and GdRhSn compounds revealed magnetic character of their ^{119}Sn spectra registered below 10 K and 16 K, respectively. Non-vanishing second and third harmonics are in agreement with ferromagnetic ordering of Nd magnetic moments in NdRhSn and with non-collinear magnetic structure of GdRhSn, which can be associated with frustration of Gd magnetic moments.

References

1. Dwight AE, Harper WC, Kimball CW (1973) HoPtSn and other intermetallic compounds with the Fe_2P -type structure. *J Less-Common Metals* 30:1–8
2. Kruk R, Kmiec R, Łatka K, Tomala K, Troć R, Tran VH (1997) Magnetic properties of UTSn compounds ($T = \text{Co}, \text{Rh}, \text{Ir}, \text{Ru}$) studied by ^{119}Sn Mössbauer spectroscopy. *Phys Rev B* 55:5851–5857
3. Łatka K, Kmiec R, Kruk R *et al.* (2003) Structure and properties of CeRhSn – a valence fluctuating system. *Acta Phys Pol B* 34:2:1225–1229
4. Mishra R, Pöttgen R, Hoffmann RD, Trill H, Mosel BD, Piotrowski H, Zumdick MF (2001) The stannides RERhSn ($\text{RE} = \text{Ho-Yb}$) and ScTSn ($T = \text{Pd}, \text{Pt}$) – structure refinements and ^{119}Sn Mössbauer spectroscopy. *Z Naturforsch B* 56:589–597
5. Routsis CD, Yakinthos JK, Gamari-Seale E (1992) Magnetic properties of the equiatomic ternary RTSn compounds ($\text{R} = \text{rare earth}, T = \text{Pt}, \text{Rh}$). *J Magn Magn Mater* 110:317–322

6. Routsis CD, Yakinthos JK, Gamari-Seale H (1992) Magnetic characteristics of some RNiSn (R = Ce, Pr, Nd, Sm) and RRhSn (R = Ce, Pr, Nd) compounds. *J Magn Magn Mater* 117:79–82
7. Sales BC, Wohleben DK (1975) Susceptibility of inter-configuration-fluctuation compounds. *Phys Rev Lett* 35:1240–1244
8. Wivel C, Mørup S (1981) Improved computational procedure for evaluation of overlapping hyperfine distributions in Mössbauer spectra. *J Phys E* 14:605–610